Removal of emerging contaminants from municipal WWTP secondary effluents by solar photocatalytic ozonation. A pilot-scale study.

Diego H. Quiñones, Pedro M. Álvarez*, Ana Rey, Fernando J. Beltrán

Departamento de Ingeniería Química y Química Física, Facultad de Ciencias, Universidad de Extremadura, Av. de Elvas s/n, 06071 Badajoz (Spain)

ABSTRACT

Ozonation, solar photocatalytic oxidation and a combination of both systems (i.e., solar photocatalytic ozonation) have been studied to treat a secondary effluent from a municipal wastewater treatment plant containing a selection of six emerging contaminants (acetaminophen, antipyrine, bisphenol A, caffeine, metoprolol and testosterone). Fe(III), Fenton reagent and TiO_2 were used in photocatalytic experiments, which were conducted in a pilot-scale compound parabolic collector photo-reactor using solar radiation as energy source. Emerging contaminants (0.2 $mg \cdot L^{-1}$ each), at pH 3, were completely removed by photo-Fenton and single ozonation in 90 and 25 min, respectively. Moreover, solar photocatalytic ozonation treatments (Fe(III)/O_3/light and Fe(III)/H_2O_2/O_3/light systems) were able to completely remove the ECs in about 20 min with UV doses of 2-6 $kJ \cdot L^{-1}$. However, the organic matter mineralization level achieved was limited (< 35% TOC removal) even after the application of solar photocatalytic ozonation, for which an enhanced generation of hydroxyl radicals was measured in experiments carried out in the presence of the hydroxyl radical probe p-chlorobenzoic acid. *Daphnia magna* bioassays were used to test toxicity of samples before and after their treatment, showing that samples subjected to solar photocatalytic ozonation were less toxic (% inhibition < 15%) than the mixture of emerging contaminants in the secondary effluent (% inhibition about 25%). Finally, a simplified estimation of operating costs shows some solar photocatalytic ozonation processes advantageous over the solar photo-Fenton system.

Keywords: Domestic wastewater, emerging contaminant, solar photocatalytic ozonation, toxicity.

***Corresponding author:** Pedro M. Álvarez

E-mail: pmalvare@unex.es; Phone: +34 924289300 (ext. 89032); Fax: +34 924289385

1. Introduction

The development of advanced analytical techniques has allowed the detection of emerging contaminants (ECs) in aquatic environments revealing a worldwide issue [1]. Many of these compounds, which are incorporated into the sewage system through domestic and industrial drains, have been found to be recalcitrant to the biological and physicochemical processes typically applied in wastewater treatment plants (WWTP). As a result, they remain in treated wastewaters being discharged into natural waters bodies (rivers, lakes, seas and streams) [1,2].

The EC group includes a wide variety of compounds such as pharmaceuticals, personal care products, hormones, industrial additives and household chemicals. Usually, their metabolites and degradation products are also included in this category of pollutants [2]. Most of the ECs are bio-accumulative, have endocrine disrupting effects and can cause health and mutagenic effects on living beings that benefit from aquatic systems [3,4].

This situation is leading to stringent regulations on wastewater management [3,5], though most of the ECs are not yet regulated [6]. Advanced oxidation processes (AOPs) can be considered as potential effective alternatives for the treatment of ECs in water. This is so because AOPs, characterized by the generation of short-life reactive species such as the hydroxyl radical ($^{\bullet}OH$), can completely degrade a wide range of water contaminants, transforming them into less harmful species. Since the application of AOPs to treat wastewaters leads to better quality effluents, wastewater recycling can be considered a management option [7].

Currently, ozonation processes are applied in wastewater treatment as disinfectant, oxidant of organic pollutants and pre or post–treatment of other unit operations (as coagulation, flocculation, biological oxidation, etc) [8].However, the use of ozone usually implies high operating costs due to its production. Moreover, although ozone itself can remove most of

the organic compounds present in domestic wastewaters, due to its selective nature, it is not usually able to mineralize them, remaining ozonation by-products in the effluents. If combined with other agents, such as UV light and/or catalysts, significant improvements in the level of organic matter mineralization and the efficiency on the use of ozone can be achieved. Such enhancements were observed in a previous work where a first approach to the application, at pilot-scale, of solar photocatalytic ozonation assisted by Fe(III), Fe(III)/H_2O_2 and TiO_2 to remove selected ECs from water was carried out [9]. As part of our continuing work on solar photocatalytic ozonation, here the treatment method has been applied to degrade ECs in a secondary effluent from a municipal WWTP. The use of solar radiation instead of UV lamps may drastically reduce the operating cost associated with the treatment system [10].

2. Materials and methods

2.1. Secondary effluent samples

First, secondary effluent samples from a municipal WWTP (Badajoz, Spain) were collected and their pH was lowered to 3 by adding concentrated hydrochloric acid solution while bubbling air to remove their carbonate and bicarbonate content, which have been found to be detrimental for the efficiency of AOPs since these species can scavenge hydroxyl radicals [11]. The main characteristics of the secondary effluent samples after this pretreatment are summarized in Table 1.

Acetaminophen (ACE), antipyrine (ANT), bisphenol A (BIS), caffeine (CAF), metoprolol (MET) and testosterone (TST), purchased from Sigma–Aldrich and used as received, were the ECs selected as target compounds for this work. Secondary effluent samples were spiked to 200 $\mu g \cdot L^{-1}$ of each compound. Additionally, p-chlorobenzoic acid (pCBA, Merck) was used as hydroxyl radical probe compound in some experiments. The chemical structures of all these compounds are shown in Fig.1.

2.2. Experimental set up and procedure

Experiments were conducted at ambient temperature in a pilot–scale solar plant located in Badajoz, Spain (38°52'43'' N, 6°58'15'' W). The solar plant consists mainly of an air compressor (Pintuc Extreme 3), an ozone generator (OZVa 1200E, ProMinent) and a compound parabolic collector (CPC, Ecosystem-Environmental Services S.A.) operated in semi-batch mode. Additionally, the plant was equipped with measurement devices (e.g., ozone analyzers) and controllers as shown in Fig.2. Thus, the CPC inlet gas stream was regulated by a precision gas flow controller (MC-10SLPM-D, Alicat Scientific) while two ozone analyzers (GM-6000-RTI and GM-6000-PRO, Anseros) were used to monitor the ozone concentration in the inlet and outlet gas streams, respectively.

The CPC used as photo-reactor consisted of four borosilicate-glass tubes (32 mm external diameter, 1.4 mm thickness, 750 mm length, ~90% transmittance) connected in series (total irradiated volume of 1.8 L) reflected by involute-type mirrors (320 G electropolished aluminum, 0.25 m^2 reflection surface), which were mounted on a fixed platform tilted 45º. The reactor also had two ports for inlet and outlet of gas, a reservoir tank of 7 L total capacity, a recirculation centrifugal pump (15-24 $L \cdot min^{-1}$), and connecting tubing and valves. The pH of the aqueous solution in the tank was automatically controlled at set-point values (i.e., 3 or 7) by an in-line pH control system provided with WP1000-P1/8S4-J4-C Welco pumps to feed hydrochloric acid or sodium hydroxide solutions to the system. The photo-reactor was also equipped with a Pt-100 probe and a broadband UV radiometer (Acadus 85-PLS) to record continuously the temperature and the incident UV radiation (λ<400 nm), respectively. Radiation data were acquired as instantaneous and accumulated UV energy (Proasis DCS-Win 3.55 software, Design Instruments S.A.). In a typical experiment, the photo-reactor reservoir tank was first loaded with 5 L of the secondary effluent containing a mixture of ECs and the required amount of catalyst (Fe(III) or TiO_2) was added afterwards. Initial concentrations of catalysts were as follows: 2.8 $mg \cdot L^{-1}$ of Fe(III) as iron(III) perchlorate

hydrate (Sigma–Aldrich) or 200 $mg \cdot L^{-1}$ of TiO_2 Aeroxide ® P25 (Evonik Industries). After adding the catalyst, the solution was recirculated through the CPC by a centrifugal pump at a flow rate of 8.7 $L \cdot min^{-1}$ so that the flux pattern inside the tubes was turbulent (Re > 7500). The CPC tubes were kept covered to avoid sunlight illumination for the first 30 min of each experiment (dark stage). This time was used for homogenization purposes and it was enough to reach the adsorption equilibria of ECs onto TiO_2 (if used). After that, the CPC was uncovered and a continuous gas flow (0.67 $L \cdot min^{-1}$ flow rate) was supplied to the reactor. Also, if needed, hydrogen peroxide (Panreac) was added at this point to the CPC system. The gas stream entering the CPC tube was either air or an ozone-air mixture (c.a. 13 $mg \cdot L^{-1}$ ozone). Experiments lasted 5 hours plus the 30 min of the dark stage. During the whole course of the experiment liquid samples were withdrawn from the reactor at intervals through a sampling port to determine the EC concentration, total organic carbon (TOC), and the concentrations of hydrogen peroxide, ozone and iron. Also, the concentration of phenolic compounds was analyzed in some liquid samples. In addition, biodegradability (i.e. the ratio between the 5-day biochemical oxygen demand and the chemical oxygen demand, BOD_5/COD ratio) and ecotoxicity (*Daphnia magna* assay) was measured in selected samples.

2.3. Analytical methods

Samples taken during the course of experiments using ozone were immediately bubbled with helium to remove residual ozone. Likewise, excess hydrogen peroxide in samples was quenched by adding an aliquot of concentrated sodium thiosulfate solution. These procedures, which did not alter the organic content of the samples, avoided further ozone and/or hydrogen peroxide reactions while samples were kept before ECs and other organic content analyses. Prior to analysis, the samples were filtered through a 0.45 µm PET filtering membrane (Chromafil Xtra). Samples used in ecotoxicity tests were withdrawn from the photo-reactor, bubbled with helium if ozone was used, mixed with catalase solution (0.1 $g \cdot L^{-1}$

bovine liver, 3390 units·mg^{-1} solid, Sigma–Aldrich) to eliminate the residual H_2O_2, neutralized and filtered through a 0.45 µm cellulose nitrate filtering membrane (Sartorius Stedim) before analysis. Samples used to analyze the dissolved ozone concentration were withdrawn from the reactor and, without any further pretreatment, analyzed immediately by the indigo method [12].

An Agilent 1100 Series HPLC (Hewlett Packard) equipped with a Kromasil C18 column (5 µm particle size, 150 mm length, 4 mm diameter, Teknokroma) as stationary phase was used to measure compounds concentration. A binary mixture of acetonitrile and 0.1% v/v phosphoric acid aqueous solution was used as mobile phase. ANT, CAF and MET were analyzed at 240, 275 and 225 nm detection wavelength, respectively, using a 15% acetonitrile mobile phase eluted at 0.65 mL·min^{-1}. BIS, TST and pCBA were analyzed at 220, 250 and 250 nm, respectively, with a 50% acetonitrile mobile phase at 1 mL min^{-1}. ACE was analyzed with a 15% acetonitrile mobile phase at 1 mL min^{-1} and 244 nm as detection wavelength. A Shimadzu TOC-V_{SCH} analyzer equipped with an infrared detector was used to measure the total, inorganic and organic carbon content. An ion chromatography apparatus (881 compact IC pro, Metrohm) equipped with a Metrosep A Supp 7 column (150 mm length, 4 mm diameter) was used to measure phosphate, sulfate, nitrate, chloride and ammonium in the secondary effluent samples. Hydrogen peroxide was measured by the Eisenberg method [13]. Total phenolic content in solution was determined by the method proposed by Singleton and Rossi [14] and expressed as mg BIS·L^{-1}. Dissolved Fe(II) was measured as indicated by Zuo [15]. COD was measured by the dichromate method using the Lange cuvette test while BOD_5 was determined measuring the oxygen consumed during a 5-day incubation period [16] using ST-OxiTop ® devices. Acute toxicity tests were conducted with Daphtoxkit F™ magna toxicity test kits (MicroBioTests) using water flea *Daphnia magna* according to OECD Guidelines [17]). pH, conductivity and turbidity of samples were measured using a GLP 21+

pHmeter (Crison), a 524 conductivity meter (Crison) and a HI 93414 turbidity meter (Hanna Instruments), respectively.

3. Results and discussion

3.1 ECs depletion and TOC removal

Samples of the MWWTP secondary effluent containing a mixture of the six above-mentioned ECs were subjected to the following treatments at pH 3: single photolysis (exposure to sunlight without reagents and/or catalyst), single ozonation in the dark (O_3), photolytic ozonation (O_3/light), Fe(III)-based photocatalytic oxidation (Fe(III)/O_2/light), Fe(III)-based photocatalytic ozonation (Fe(III)/O_3/light), photo-Fenton (Fe(III)/H_2O_2/O_2/light) and photo-Fenton-based photocatalytic ozonation (Fe(III)/H_2O_2/O_3/light). For comparison purposes, also TiO_2-based photocatalytic oxidation (TiO_2/O_2/light), TiO_2 photocatalytic ozonation (TiO_2/O_3/light) and ozonation (O_3) processes were applied at pH 7.

Single photolysis was not able to degrade the ECs. Thus, only TST was removed to some extent by single photolysis (34% removal after 5h irradiation, which meant 33 kJ·L^{-1} UV radiation supplied). Fe(III) photocatalytic oxidation experiments only led to EC removal percentages between 26% (ANT) and 43% (TST) after 5 h treatment (39 kJ·L^{-1} UV radiation dose). However, complete removal of ECs was achieved in photo-Fenton experiments in less than 90 min reaction time (8 kJ·L^{-1} UV radiation dose) and in single ozonation experiments at pH 3 and 7 in about 25 min (c.a. 28 mg O_3·L^{-1}) and 45 min (c.a. 100 mg O_3·L^{-1}), respectively. Moreover, systems involving ozone and solar radiation (i.e. O_3/light, Fe(III)/O_3/light and Fe(III)/H_2O_2/O_3/light) where able to eliminate, at pH 3, the ECs faster (20-30 min) and with UV doses lower than 6 kJ·L^{-1}. Among them, the Fe(III)/H_2O_2/O_3/light system was observed to be the most efficient, leading to complete removal of ECs with UV radiation and ozone doses of about 2 kJ·L^{-1} and 19 mg L^{-1}, respectively. TiO_2 photocatalytic experiments, carried out at pH 7, also led to the complete disappearance of the ECs but they required higher UV

radiation doses than photo-Fenton and photocatalytic ozonation experiments performed at pH 3. Thus, TiO_2 photocatalytic oxidation experiments (TiO_2/O_2/light) absorbed about 15 $kJ \cdot L^{-1}$ of UV radiation (c.a. 2 h of irradiation) to eliminate the parent ECs while in TiO_2/O_3/light experiments the consumptions of UV light and ozone were about 12 $kJ \cdot L^{-1}$ and 37 mg L^{-1}, respectively (c.a. 40 min of simultaneous irradiation and ozonation).

Fig.3 shows a comparison of the efficiency of some of the solar treatment systems applied in this work in terms of the use of radiation to remove the selected ECs. The delivered UV radiation per volume unit, $Q_{UV,n}$, as represented in Fig.3**,** has been computed using the Eq.(1) [18]**:**

$$Q_{UV,n} = Q_{UV,n-1} + \left(t_n - t_{n-1}\right)\overline{UV}_{G,n}\frac{A}{V} \quad (1)$$

where t_n is the elapsed irradiation time until sample n, $\overline{UV}_{G,n}$ is the average incident UV radiation in the period $t_{n-1} - t_n$, V is the total reaction volume and A is the illuminated reactor surface. As it can be seen in Fig.3, the treatment systems involving ozone were the most efficient in removing the selected ECs while the Fe(III)/O_2/light system was the one that required the highest UV radiation dose to remove the ECs. Also, it is apparent from Fig.3 that, in all cases, the ECs depletion profiles followed a pseudo first-order kinetics with respect to the UV radiation dose. Accordingly, Eq.(2) was satisfactory fulfilled:

$$\ln\left(\frac{\Sigma C_{EC,0}}{\Sigma C_{EC}}\right) = k_{UV}Q_{UV} \quad (2)$$

The value of the pseudo first-order rate constant, $k_{UV,}$ was used to estimate the time required to remove 99% of the initial concentration of ECs (t_{99}) at a given average incident UV irradiation ($\overline{UV}_G$). Thus, Eq.(3) was applied:

$$t_{99} = \frac{\ln(100)}{k_{UV}} \frac{V}{\overline{UV}_G \, A} \quad (3)$$

where A and V are the reactor irradiation area and the reaction volume, respectively. Experimental data from single ozonation experiments, carried out in absence of radiation, were satisfactorily fitted to Eq.(4):

$$\ln\left(\frac{\Sigma C_{EC,0}}{\Sigma C_{EC}}\right) = k\,t \quad (4)$$

where k is the apparent pseudo first-order rate constant for total EC depletion and t is the irradiation time. In accordance with this, t_{99} was estimated by the expression (5):

$$t_{99} = \frac{\ln(100)}{k} \quad (5)$$

Table 2 shows the values of the pseudo first-order rate constants for the various treatment systems derived from experimental data (for conditions see the legend of Fig.3) and t_{99} values computed either by Eq.(3) considering an average incident UV irradiation of 30 $W \cdot m^{-2}$, which is the typical average UV flux in a sunny day [18] or by Eq.(5).

As far as TOC removal is concerned, Fig.4 shows, for selected experiments, the evolution of TOC conversion as a function of the UV radiation supplied. It should be mentioned here that the overall TOC in the wastewater samples subjected to treatment was composed of TOC from occurring compounds in the secondary effluent (average TOC = 20 $mg \cdot L^{-1}$) and TOC from added ECs (TOC = 0.8 $mg \cdot L^{-1}$). Accordingly, about 96% of TOC in the samples to be treated was due to the organics present in the MWWTP secondary effluent. As it can be observed in Fig.4, TOC removal was far from being complete (<35% TOC removal) in any of the experiments carried out despite the high average incident radiation, which was ranged between 35 and 46 $W \cdot m^{-2}$ (i.e., cumulative UV radiation dose in 5-h experiments was higher

than 30 $kJ \cdot L^{-1}$). Nevertheless, it should be mentioned that COD removals (up to 70%) were greater than TOC removals in all cases. Thus, the COD/TOC ratio decreased from the initial value of about 3 to final values of 1.5-2, suggesting that the oxidation progressed to yield organic products which were recalcitrant and, therefore, difficult to degrade. Under the experimental conditions applied in this work, low TOC removal (< 5%) was observed after the application of ozonation in the dark (O_3), both at pH 3 and 7, and the Fe(III)/O_2/light (pH 3) system (results not shown). Photocatalytic ozonation systems (i.e., Fe(III)/O_3/light and Fe(III)/H_2O_2/O_3/light) at pH 3, however, were much more effective leading to 20-35% TOC conversion (see Fig.4). In TiO_2 photocatalytic experiments (pH 7), it was observed an initial period where the TOC removal negligible followed by a period of higher TOC conversion up to reach 8% (TiO_2/O_2/light) and 20% (TiO_2/O_3/light) removals after the 5-h treatment. The induction period in TiO_2 catalytic systems could be ascribed to the formation of agglomerates of catalyst crystallites or to the adsorption of some inorganic ions on the catalyst surface [19].

For comparative purposes, TOC experimental data were fitted to a first-order kinetic equation. Fig.5 shows the apparent first-order rate constant, $k_{TOC,app}$, computed for some of the systems applied as well as the average incident radiation measured during each experiment. As it can be deduced from Fig.5, the mineralization (i.e., TOC removal) rate constants followed the order: Fe(III)/H_2O_2/O_3/light (pH 3) > Fe(III)/O_3/light (pH 3) > Fe(III)/H_2O_2/O_2/light (pH 3) > TiO2/O_3/light (pH 7) > TiO_2/O_2/light (pH 7). Single ozonation (pH 3 and 7), single photolysis (pH 3) and Fe(III)/O_2/light (pH 3) experiments led to very low values of $k_{TOC,app}$ (< 5×10^{-4} min^{-1}) as limited TOC removal (< 5%) was observed after the 5-h experiments. The Fe(III)/H_2O_2/O_3/light system, which showed the highest mineralization rate constant, was also the most efficient system in terms of use of energy (7.5 kJ per mg of TOC removed). Fe(III)/O_3/light (pH 3) and TiO_2/O_3/light (pH 7) experiments showed similar energy efficiencies, ranging between 14.5 and 16.8 kJ per mg of TOC removed. Accordingly, these systems led to similar mineralization degrees (19-23% TOC removal). Photocatalytic

oxidation systems such as Fe(III)/H_2O_2/O_2/light (pH 3) and TiO_2/O_2/light (pH 7) required more UV energy to remove each mg of TOC (90 and 35 kJ·mg^{-1}, respectively) and led to lower mineralization levels (6-9% TOC removal) than the photocatalytic ozonation systems tested.

3.2 Hydroxyl radical exposure

In the applied AOPs, the depletion of the pollutants might take place mainly by three pathways: photolysis, direct reaction with molecular ozone and oxidation by hydroxyl radicals. Taking into account those contributions, the degradation of each compound can be expressed by Eq.(6):

$$\frac{dC_{EC}}{dt} = -\left(k_{phot.} + k_{OH}C_{OH} + k_{O3}C_{O3}\right)C_{EC} \quad (6)$$

In Eq(6), $k_{phot.}$ is the first order rate constant for compound photolysis, $k_{OH\text{-}EC}$ and $k_{O3\text{-}EC}$ are the rate constants for the reaction of each EC with the hydroxyl radical and dissolved ozone, respectively; C_{EC}, C_{OH} and C_{O3} are the concentration of EC, hydroxyl radical and ozone, respectively. After integration and variable separation, the following expression is obtained:

$$\ln\left(\frac{C_{EC,0}}{C_{EC}}\right) = k_{phot.}\int_0^t dt + k_{OH}\int_0^t C_{OH}dt + k_{O3}\int_0^t C_{O3}dt \quad (7)$$

where $\int C_{OH}\,dt$ and $\int C_{O3}\,dt$ are the corresponding hydroxyl radicals and ozone exposures.

Hydroxyl radical exposure is thought to have a high impact on the mineralization of organic compounds in the secondary effluent (both added ECs and naturally occurring compounds) through the AOPs studied because direct photolysis and single ozonation at pH 3, where low concentration of $^{\bullet}OH$ is expected, did not lead to significant TOC removals (< 2%).

The hydroxyl radical exposure can be calculated using pCBA as a probe compound [20] because of its high reactivity with $^{\bullet}OH$ (k_{OH} = 5 x 10^9 L·mol^{-1}·s^{-1} [21]) and negligible reactivity

with ozone (k_{O3} < 0.15 $L \cdot mol^{-1} \cdot s^{-1}$ [22]). In addition, aqueous pCBA does not absorb radiation beyond 290 nm wavelength and, therefore, pCBA does not undergo direct photolysis under solar irradiation (i.e., $k_{phot} \sim 0$). Accordingly, the •OH exposure can be calculated by Eq.(8):

$$\int_0^t C_{OH} dt = \frac{\ln\left(\frac{C_{pCBA,0}}{C_{pCBA}}\right)}{k_{OH}} \quad (8)$$

Table 3 summarizes the •OH exposure during the first minutes of experiments of degradation of ECs in the secondary effluent in the presence of pCBA. It can be seen that the •OH exposure increased with the UV radiation dose for any of the system tested. For a given radiation dose, the ozone/light systems (pH 3) led to higher •OH production than those systems carried out in the absence of ozone. The Fe(III)/H_2O_2/O_3/light (pH 3) system can be highlighted as that leading to the highest •OH exposure and, as a result, the highest TOC removal after 5-h treatment (35%).

3.3 Phenolic intermediates

Given the molecular structures of the selected ECs (see Fig.1) as well as those of other organic compounds typically present in MWWTP secondary effluents, some of the primary intermediates expected to be formed during their oxidation are phenolic compounds. Fig. 6 shows the evolution of the concentration of phenolic compounds during the course of selected experiments. As can be seen, during the first minutes of reaction, an increase in the phenolic compounds concentration was observed in Fe(III)/O_2/light (pH 3) and TiO_2/O_2/light (pH 7) experiments, which clearly indicates that rates of formation of these species are higher than rates of consumption. As shown in Table 3, these systems are, among the studied, those that led to the lowest hydroxyl radical exposures and, as a consequence, showed the lowest organic matter degradation rates. Thus, accumulation of phenolic intermediates was more pronounced during the course of these experiments. On the other

hand, photolytic ozonation and photocatalytic ozonation systems, which led to the formation of hydroxyl radicals to a significant extent (see Table 3), were more effective in removing the phenolic content of samples. Thus, no accumulation of phenolic substances was observed throughout the course of these experiments and percentages of removal after the 5-h experiments were around 60-75% as it is apparent from Fig. 6. The Fe(III)/H_2O_2/O_2/light (pH 3) system was also able to remove phenolic compounds to some extent, though no more than 30% removal was achieved after 5 hours of experiment. Finally, single ozonation systems (pH 3 and 7, not shown in Fig. 6) led to 45-50% removal of the initial phenolic content after 5 h of treatment.

3.4 Biodegradability measurements

The BOD_5/COD ratio in samples before and after the experiments was measured to assess changes in biodegradability. It was found that samples taken after the 5-h experiments had BOD_5/COD ratios ranged from 0.15 to 0.47. Since the initial BOD_5/COD value was 0.17 (see Table 1), it can be concluded that, in general, the AOPs tested enhanced the biodegradability of samples. Particularly, the Fe(III)/H_2O_2/O_3/light (pH 3) system led to a 2.5-fold increase of the BOD_5/COD ratio.

3.5 Toxicity tests

One important aspect about the application of AOPs is the possible formation of toxic intermediates or by-products, which could be even more toxic than the compounds initially present in the samples. Toxicity bioassays of some selected reaction samples were carried out using acute *Daphnia magna*. For this purpose, samples were taken from the reactor at a time when complete ECs removal was almost achieved (i.e, t_{99} as defined in equations (3) or (5)) and after the 5-h experiments. Table 4 shows the results of immobilization of *Daphnia magna* after 48 hours exposure. It should be mentioned here that no data for t_{99} were obtained for the Fe(III)/O_2/light (pH 3) system since no complete removal of ECs could be

achieved after 5 hours of application of this treatment (see Table 2). The results of toxicity bioassays showed an increase of toxicity after the addition of ECs to the secondary effluent. Thus, the percentage of inhibition increased from 5% (without added ECs) to about 25% (second column (t=0) in Table 4). Also, changes in sample toxicity were observed during the course of the photocatalytic experiments. As a rule, toxicity of samples increased at the beginning of the photocatalytic treatment, likely as a consequence of the accumulation of phenolic and other toxic intermediates and then decreased. This result is in agreement with that reported for the removal of other ECs by ozonation and solar photocatalytic oxidation with TiO_2 [23,24]. Toxicity removal below the baseline level (c.a., 25% inhibition) was only observed when a large degree of TOC removal (i.e., mineralization) was achieved. This applies especially for the Fe(III)/O_3/light (pH 3) and Fe(III)/H_2O_2/O_3/light (pH 3) photocatalytic ozonation systems.

3.6 Influence of the H_2O_2/Fe(III) ratio

The Fe(III)/H_2O_2/O_3/light treatment at pH 3 has been proved so far as a good choice for the treatment of the secondary effluent contaminated with the ECs, as complete removal of ECs, high mineralization of organic matter (i.e., 35 % TOC removal) and great removal of phenolic compounds (i.e., 71% removal) were achieved after 5 h of treatment (i.e., 38.7 $kJ \cdot L^{-1}$ radiation dose). In addition, the effluent from the treatment did not show toxicity towards *Daphnia magna* (i.e., < 5% inhibition) and presented a favourable BOD_5/COD ratio. A key parameter of the process performance and the process efficiency for this AOP is the H_2O_2/Fe(III) ratio. To study the effect of this variable a series of experiments were carried out at varying mass ratios in the range 6.1-18.3. Following results of Table 5, where some process performance parameters are presented, the best H_2O_2/Fe(III) mass ratio, in the range considered here, was 12.2. Although, the greater H_2O_2/Fe(III) ratio the faster EC removal observed (i.e., lower t_{99}), the TOC removal rate was the highest when applying a 12.2 H_2O_2/Fe(III) mass ratio. The lower TOC removal rate obtained at the highest

H_2O_2/Fe(III) mass ratio compared to the optimum is likely to be a consequence of the hydroxyl radical scavenger character of hydrogen peroxide.

3.7 Simplified comparison of operating costs

Operating an efficient and cost-effective treatment process is the goal of every successful MWWTP. Therefore, before process development and scale-up economic analysis must be considered. In this work a simplified economic comparison of operating costs associated with the investigated treatment process is presented. The economic analysis accounts for the costs of the main reagents and/or catalysts used (i.e., iron (III), hydrogen peroxide and titanium dioxide) according to vendors (Proquiman and Quimidroga, Spain) as well as that of the electricity (Red Eléctrica de España, Spain) to power the air compressor, the ozone generator and the CPC reactor of the pilot-plant used in this work. Pre-treatment costs (e.g., pH adjustment) have not been accounted for. As basis for the evaluation, experimental conditions used throughout this investigation have been considered. Also, two criteria have been used: (1) operating costs to reach complete removal of ECs; (2) operating costs to remove 20% of the TOC of the secondary effluent. Results are shown, as relative cost, in Table 6. Relative cost of the solar photo-Fenton process has been set as 1 as this system is, so far, the best known solar photoctalalytic treatment process. Recently, Durán and co-workers [25] estimated an operating cost of 1.56 €·m^{-3} for the treatment of a secondary effluent from a MWWTP contaminated with antipyrine by a solar poto-Fenton method at semi-industrial scale. In the present work, the operating cost of the solar photo-Fenton process was found to be 0.80 or 1.68 €·m^{-3} depending on whether the treatment objective was the complete removal of ECs or the reduction of TOC by a 20%. From the results of Table 6, it is apparent that the systems which involve the use of ozone, except the TiO_2/O_3/light (pH 7) system, are the most economic choices when the goal is just the 99% removal of the ECs, with relative costs ranging from 0.32 to 0.38. On the other hand, the operating cost of the Fe(III)/O_2/light (pH 3) system is the highest due to the long treatment

time needed to remove the ECs (see Table 2). If the treatment goal is also the removal of TOC to some extent (i.e., 20% TOC removal) the solar photocatalytic ozonation systems using iron or iron and H_2O_2 have the lowest operating costs while the use of TiO_2 as catalyst increases significantly the cost due to the expensiveness of this material.

4. Conclusions

From the results of this study, it can be concluded that iron-mediated solar photocatalytic ozonation can be a suitable method to degrade ECs in secondary effluents from MWWTPs. The ECs used in this investigation (acetaminophen, antipyrine, bisphenol A, caffeine, metoprolol and testosterone) were easily removed by ozone but the organic matter in the effluent was difficult to mineralize at the experimental conditions applied. Thus, TOC conversion was found lower than 35% after 5 h of treatment. In any case, solar photocatalytic ozonation processes were shown to be more efficient than single ozonation and single photocatalytic oxidation systems in terms of TOC removal due to an enhanced generation of hydroxyl radicals. Treated effluents after the application of solar photocatalytic ozonation showed low toxicity towards *Daphnia magna* (inhibition percentage < 15%, while the non-treated secondary effluent showed about 25% inhibition) and higher biodegradability (BOD_5/COD ratio = 0.15-0.47) than the non-treated secondary effluent. Finally, a simplified estimation of operating costs revealed that some solar photocatalytic ozonation processes (e.g., Fe(III)/O_3/light and Fe(III)/H_2O_2/O_3/light) can be cheaper than the solar photo-Fenton system.

Acknowledgements

This study was supported by Spanish Ministerio de Economía y Competitividad (MINECO) and European Regional Development Funds through the projects CTQ2009/13459-C05-05 and CTQ2012-35789-C02-01. D. H. Quiñones is grateful to MINECO for the concession of a predoctoral FPI grant.

1 **References**

[1] M. Stuart, D. Lapworth, E. Crane, A. Hart, Review of risk from potential emerging contaminants in UK groundwaters, Sci. Total Environ., 446 (2012) 1–21.

[2] C. Mukhopadhyay, A. Mason, Smart Sensors for Real-Time Water Quality Monitoring, Springer, New York, 2013.

[3] T. Deblonde, C. Cossu-Leguille, P. Hartemann, Emerging pollutants in wastewater: A review of the literature, Int. J. Hyg. Environ. Health 214 (2011) 442–448.

[4] N. Bolong, A.F. Ismail, M.R. Salim, T. Matsuura, A review of the effects of emerging contaminants in wastewater and options for their removal, Desalination 239 (2009) 229–246.

[5] M.H.Y. Lau, K.M.Y. Leung, S.W.Y Wong, H. Wang, Z.G. Yan, Environmental policy, legislation and management of persistent organic pollutants (POPs) in China, Environ. Pollut. 165 (2012) 182-192.

[6] P. Verlicchi, A. Galletti, M. Petrovic, D. Barceló, Hospital effluents as a source of emerging pollutants: An overview of micropollutants and sustainable treatment options, J. Hydrol. 389 (2010) 416-428.

[7] Z. Liu, Y. Kanjo, S. Mizutani, Removal mechanisms for endocrine disrupting compounds (EDCs) in wastewater treatment — physical means, biodegradation, and chemical advanced oxidation: A review, Sci. Total Environ. 407 (2009) 731-748.

[8] F.J. Beltrán, Ozone reaction kinetics for water and wastewater systems, Lewis Publishers, CRC Press. Boca Raton, Florida, EEUU, 2003.

[9] D.H. Quiñones, P.M. Álvarez, A. Rey, S. Contreras, F. J. Beltrán, Application of solar photocatalytic ozonation for the degradation of emerging contaminants in water in a pilot plant, Chem. Eng. J. 260 (2015) 399–410.

[10] L. Prieto-Rodríguez, I. Oller, N. Klamerth, A. Agüera, E.M. Rodríguez, S. Malato, Application of solar AOPs and ozonation for elimination of micropollutants in municipal wastewater treatment plant effluents, Water Res. 15 (2013) 1521-1528.

[11] I. Gultekin, N.H. Ince, Degradation of reactive azo dyes by UV/H_2O_2: impact of radical scavengers, J. Environ. Sci. Health A Tox Hazard Subst Environ Eng. 39 (2004) 1069-1081.

[12] H. Bader, J. Hoigné, Determination of ozone in water by the indigo method, Water Res. 15 (1981) 449–456.

[13] G. Eisenberg, Colorimetric Determination of hydrogen peroxide, Ind. Eng. Chem. Anal. Ed. 15 (1943) 327–328.

[14] V. Singleton, J. Rossi, Colorimetry of total phenolic with phosphomolybdic-phosphotungstic acid reagents, Am. J. Enol. Viticult. 16 (1965) 144-158.

[15] Y. Zuo, Kinetics of photochemical/chemical cycling of iron coupled with organic substances in cloud and fog droplets, Geochim. Cosmo. Chim. Ac. 59 (1995) 3123-3130.

[16] APHA-AWWA-WEF. *5210B: Biochemical Oxygen Demand (BOD), Standard methods for the examination of water and wastewater*. 21th Edition. (2005) Washington DC.

[17] OECD. Test No. 202: Daphnia sp. Acute immobilisation test, OECD Guidelines for the testing of chemicals, Section 2, OECD Publishing, 2004.

[18] S. Malato, J. Blanco, A. Vidal, D. Alarcón, M.I. Maldonado, J. Cáceres, W. Gernjak, Applied studies in solar photocatalytic detoxification: an overview, Sol. Energy, 75 (2003) 329–336.

[19] E. V. Savinkina, L. N. Obolenskaya, G. M. Kuz'micheva, A. V. Dorokhov, A. Yu. Tsivadze, A new η-titania-based photocatalyst, Dokl. Phys. Chem. 441 (2011) 224-226

[20] M.S. Elovitz, U. von Gunten, Hydroxyl radical/ozone ratios during ozonation processes. I. The R_{ct} concept, Ozone Sci. Eng. 21 (1999) 239–260.

[21] G.V. Buxton, C.L. Greenstock, W.P. Helman, A.B. Ross, Critical review of rate constants for reactions of hydrated electrons, hydrogenatoms and hydroxyl radicals in aqueous solution, J. Phys. Chem. Ref. Data 17 (1988) 513-886.

[22] D.C.C. Yao, W.R. Haag, Rate constants for direct reactions of ozone with several drinking water contaminants, Water Res. 25 (1991) 761–773.

[23] G. Márquez, E.M. Rodríguez, F.J. Beltrán, P.M. Álvarez, Solar photocatalytic ozonation of a mixture of pharmaceutical compounds in water, Chemosphere 113 (2014) 71-78.

[24] G. Márquez, E.M. Rodríguez, M. I. Maldonado, P.M. Álvarez, Integration of ozone and solar TiO_2-photocatalytic oxidation for the degradation of selected pharmaceutical compounds in water and wastewater, Sep. Purif. Technol. 136 (2014) 18-26.

[25] A. Durán, J.M. Monteagudo, I. Sanmartín, A. Valverde, Solar photodegradation of antipyrine in a synthetic WWTP effluent in a semi-industrial installation, Sol. Energ. Mat. Sol. C. 125 (2014) 215-222.

Tables

List of tables:

Table 1. Main characteristics of the secondary effluent samples used in this work (after pH adjustment treatment)

Parameter	Value
Inorganic carbon (mg L^{-1})	0.3±0.2
Total organic carbon (mg L^{-1})	20.0±2.1
pH	3.0±0.1
BOD_5 (mg L^{-1})	10±3
COD (mg L^{-1})	58.6±3.5
Turbidity (NTU)	7.8±1.1
Conductivity (µS cm^{-1})	1330±9
PO_4^{3-} (mg L^{-1})	10.4±1.0
SO_4^{2-} (mg L^{-1})	63.6±0.5
Cl^- (mg L^{-1})	295.7±4.6
NH_4^+ (mg L^{-1})	2.5±0.6
NO_3^- (mg L^{-1})	5.7±0.8

Table 2. Pseudo first-order rate constants and estimated depletion time for 99% total EC concentration removal for the AOPs studied in this work.

AOP	k_{UV} (L·kJ^{-1}) [a] or k (min^{-1}) [b]	t_{99} (min)
O_3/light/pH 3	1.438[a]	36[c]
Fe(III)/O_2/light/pH 3	0.021[a]	2344[c]
Fe(III)/O_3/light/pH 3	1.476[a]	35[c]
Fe(III)/H_2O_2/O_2/light/pH 3	0.325[a]	158[c]
Fe(III)/H_2O_2/O_3/light/pH 3	1.501[a]	34[c]
TiO_2/O_2/light/pH 7	0.258[a]	198[c]
TiO_2/O_3/light/pH 7	0.975[a]	60[c]
O_3/pH 3	0.110 [b]	42[d]
O_3/pH 7	0.069 [b]	67[d]

[a] Calculated by equation (2); [b] Calculated by equation (4); [c] Calculated by equation (3), assuming UV_G=30 W m^{-2}, V = 5 L and A = 0.25 m^2; [d] Calculated by equation (5)

Table 3. Hydroxyl radical exposures ($\int C_{HO\cdot}$ dt, M·s) observed in experiments of degradation of ECs in the secondary effluent by different AOPs [(a)]

UV radiation dose applied ($kJ \cdot L^{-1}$)	1.0	2.5	5.0
AOP	**$\int C_{HO\cdot} dt \times 10^{10}$**	**$\int C_{HO\cdot} dt \times 10^{10}$**	**$\int C_{HO\cdot} dt \times 10^{10}$**
Fe(III)/O_2/light/pH 3	0.16	0.35	0.40
TiO_2/O_2/light/pH 7	0.11	0.58	1.34
Fe(III)/H_2O_2/O_2/light/pH 3	0.62	1.12	1.63
TiO_2/O_3/light/pH 7	0.50	2.05	2.27
O_3/light/pH 3	0.37	1.32	3.97
Fe(III)/O_3/light/pH 3	0.41	1.24	4.36
Fe(III)/H_2O_2/O_3/light/pH 3	0.85	2.68	5.47

[(a)] For experimental AOP conditions see Fig. 3.

Table 4. Toxicity towards *Daphnia magna* of reaction samples from experiments of degradation of ECs in the secondary effluent by different AOPs [(a)]

Reaction time	0	t_{99}	5 h
AOP	**Percentage inhibition (%)**		
Fe(III)/O_2/light/pH 3	25	NM	30
TiO_2/O_2/light/pH 7	21	31	26
Fe(III)/H_2O_2/O_2/light/pH 3	24	18	9
TiO_2/O_3/light/pH 7	27	32	14
O_3/light/pH 3	24	44	33
Fe(III)/O_3/light/pH 3	28	33	5
Fe(III)/H_2O_2/O_3/light/pH 3	25	38	2

$t_{99=}$ time needed to reach 99% removal of ECs; NM= not measured as t_{99} was greater than 5 h.
[(a)] For experimental AOP conditions see Fig. 3.

Table 5. Effect of the H_2O_2/Fe(III) ratio on the performance of the Fe(III)/H_2O_2/O_3/light treatment at pH 3

H_2O_2/Fe(III) mass ratio	6.1	12.2	18.3
$k_{TOC} \times 10^3$ (min^{-1})	3.01	3.32	2.58
% TOC removal	35	42.6	39.6
% Phenolic compounds removal	70.8	75.4	73.1
UV radiation dose ($kJ \cdot L^{-1}$)	38.7	24.3	28.6
t_{99} (min)	34	22	18

Experimental conditions: EC concentration= 200 μg L^{-1}, each; Applied ozone = 520 mg h^{-1}; $C_{Fe(III),0}$ = 2.8 mg L^{-1}; Overall radiation dose ~30 kJ L^{-1}; Treatment time = 5 h.

Table 6. Estimated relative operating costs of the AOPs studied at pilot-plant scale.

Treatment system	Relative cost	
	Objective: Complete EC removal	Objective: 20% TOC removal
O_3/light/pH 3	0.32	0.62
Fe(III)/O_3/light/pH 3	0.32	0.46
Fe(III)/H_2O_2/light/pH 3	1.00	1.00
Fe(III)/O_2/light/pH 3	14.28	*
O_3/pH 3	0.38	*
Fe(III)/H_2O_2/O_3/light/pH 3	0.35	0.44
TiO_2/light/pH 7	2.57	1.92
TiO_2/O_3/light/pH 7	1.88	1.25

Notes: Fe(III)/H_2O_2/O_2/light has been chosen as reference system (relative cost = 1); Experimental conditions as indicated in Fig.3.

(*) Not calculated, as very low mineralization (< 2.5%) was achieved in 5 hours by the treatment method at the conditions applied.

Figures

Figure captions:

Fig. 1. Chemical structures of the chemical compounds used in this work

Fig. 2. Simplified scheme of the solar pilot plant used in this work

Fig.3. Plot of $\Sigma C_{ECs,0}/\Sigma C_{ECs}$ against the UV radiation dose (Q_{UV}) for some experiments. Experimental conditions: EC concentration= 200 μg L^{-1}, each; Applied ozone = 520 mg h^{-1}; $C_{Fe(III),0}$ = 2.8 mg L^{-1}; Initial H_2O_2/Fe(III) mass ratio = 6.1; $C_{TiO2,0}$ = 200 mg L^{-1}. Symbols: (◍) O_3/light/pH 3, (○) Fe(III)/O_2/light/pH 3, (◇) Fe(III)/O_3/light/pH 3, (▣) Fe(III)/H_2O_2/O_2/light/pH 3, (▲) Fe(III)/H_2O_2/O_3/light/pH 3, (△)TiO_2/O_2/light/pH 7, (●) TiO_2/O_3/light/pH 7. Lines: linear regression (R^2>0.96)

Fig. 4. TOC removal vs UV energy dose for some experiments. Experimental conditions: EC concentration= 200 μg L^{-1}, each; Applied ozone = 520 mg h^{-1}; $C_{Fe(III),0}$ = 2.8 mg L^{-1}; Initial H_2O_2/Fe/(III) mass ratio = 6.1; $C_{TiO2,0}$ = 200 mg L^{-1}.

Fig.5. Apparent mineralization rate constant and average incident radiation for some experiments. Experimental conditions: EC concentration= 200 μg L^{-1}, each; Applied ozone = 520 mg h^{-1}; $C_{Fe(III),0}$ = 2.8 mg L^{-1}; Initial H_2O_2/Fe/(III) mass ratio = 6.1; $C_{TiO2,0}$ = 200 mg L^{-1}.

Fig.6. Evolution of the phenolic concentration with the dose of UV radiation during the course of some photocatalytic experiments. Experimental conditions: EC concentration= 200 μg L^{-1}, each; Applied ozone = 520 mg h^{-1}; $C_{Fe(III),0}$ = 2.8 mg L^{-1}; Initial H_2O_2/Fe/(III) mass ratio = 6.1; $C_{TiO2,0}$ = 200 mg L^{-1}. Symbols: (◍) O_3/light/pH 3, (○) Fe(III)/O_2/light/pH 3, (◇) Fe(III)/O_3/light/pH 3, (▣) Fe(III)/H_2O_2/O_2/light/pH 3, (▲) Fe(III)/H_2O_2/O_3/light/pH 3,(△) TiO_2/O_2/light/pH 7, (●) TiO_2/O_3/light/pH 7

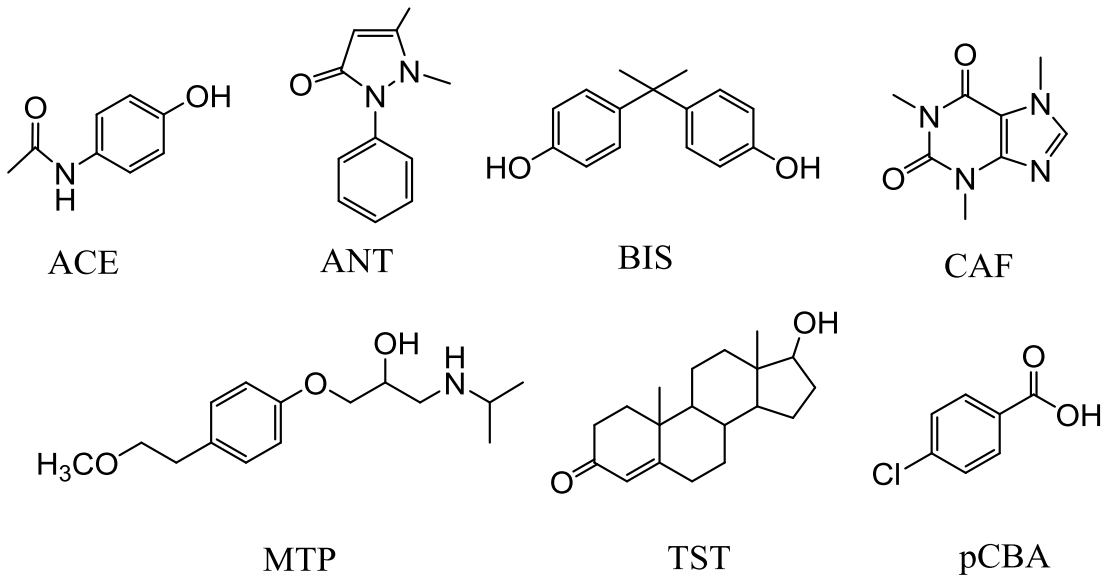

Fig.1. Chemical structures of the chemical compounds used in this work

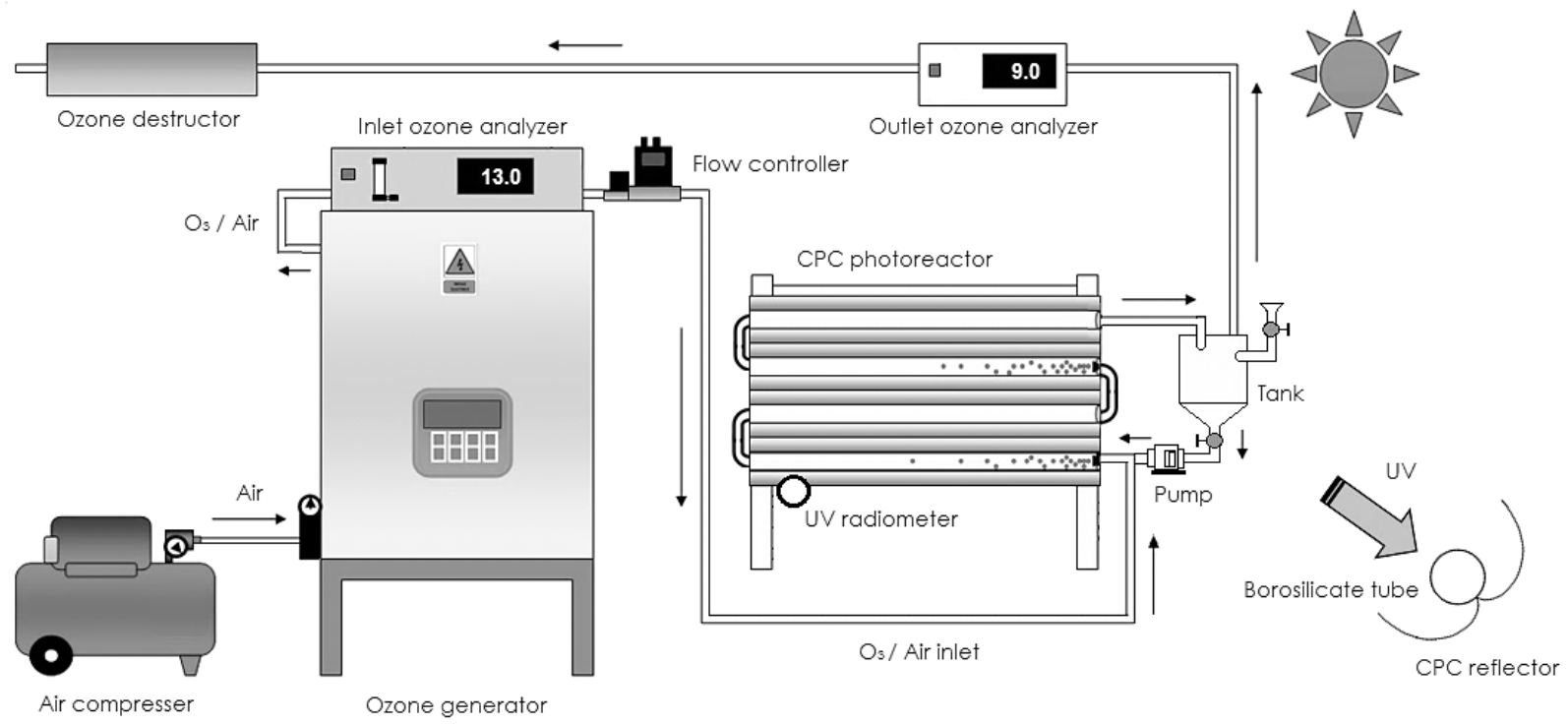

Fig. 2. Scheme of the solar pilot plant used in this work

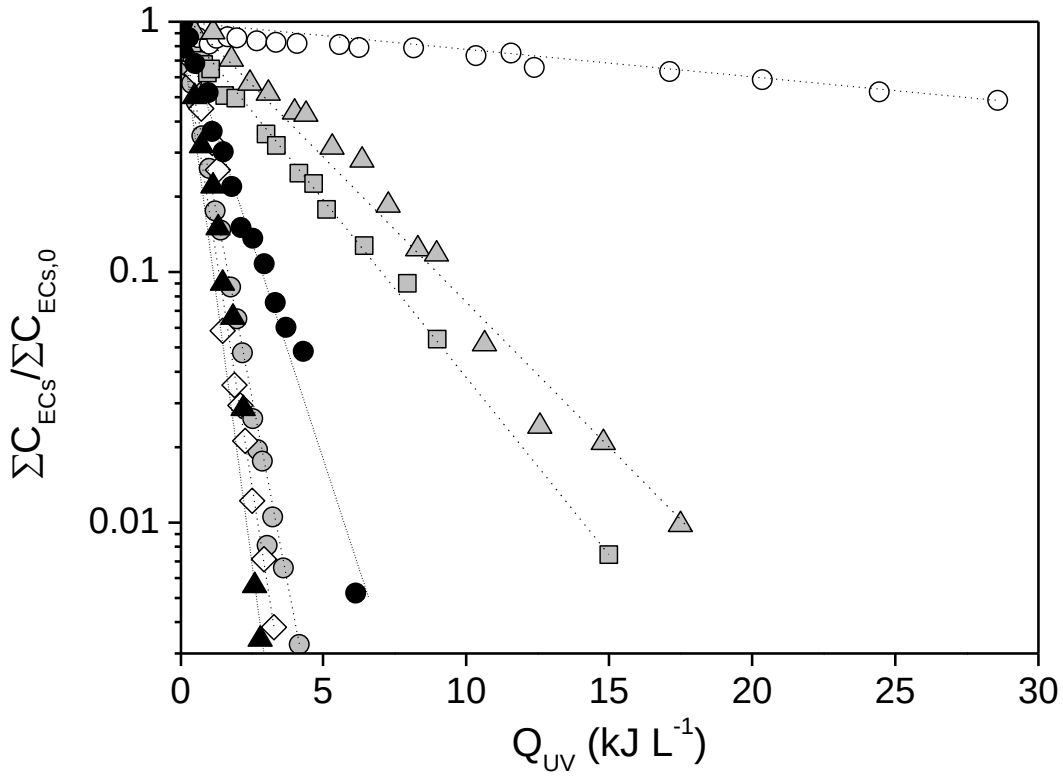

Fig.3. Plot of $\Sigma C_{ECs,0}/\Sigma C_{ECs}$ against the UV radiation dose (Q_{UV}) for some experiments. Experimental conditions: EC concentration= 200 μg L^{-1}, each; Applied ozone = 520 mg h^{-1}; $C_{Fe(III),0}$ = 2.8 mg L^{-1}; Initial H_2O_2/Fe(III) mass ratio = 6.1; $C_{TiO2,0}$ = 200 mg L^{-1}. Symbols: (◍) O_3/light/pH 3, (○) Fe(III)/O_2/light/pH 3, (◇) Fe(III)/O_3/light/pH 3, (▣) Fe(III)/H_2O_2/O_2/light/pH 3, (▲) Fe(III)/H_2O_2/O_3/light/pH 3, (△)TiO_2/O_2/light/pH 7, (●) TiO_2/O_3/light/pH 7. Lines: linear regression (R^2>0.96)

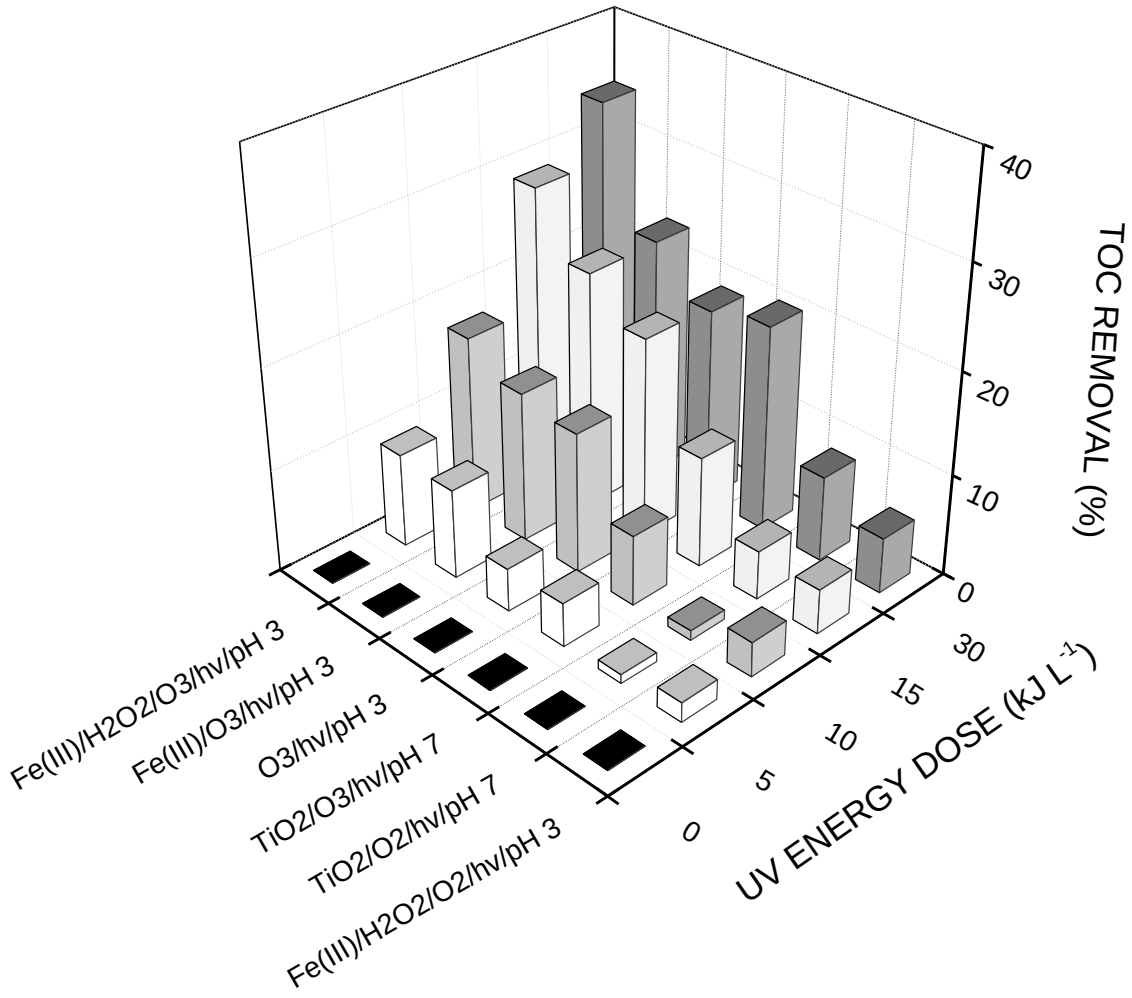

Fig.4. TOC removal vs UV energy dose for some experiments. Experimental conditions: EC concentration= 200 µg L^{-1}, each; Applied ozone = 520 mg h^{-1}; $C_{Fe(III),0}$ = 2.8 mg L^{-1}; Initial H_2O_2/Fe/(III) mass ratio = 6.1; $C_{TiO2,0}$ = 200 mg L^{-1}.

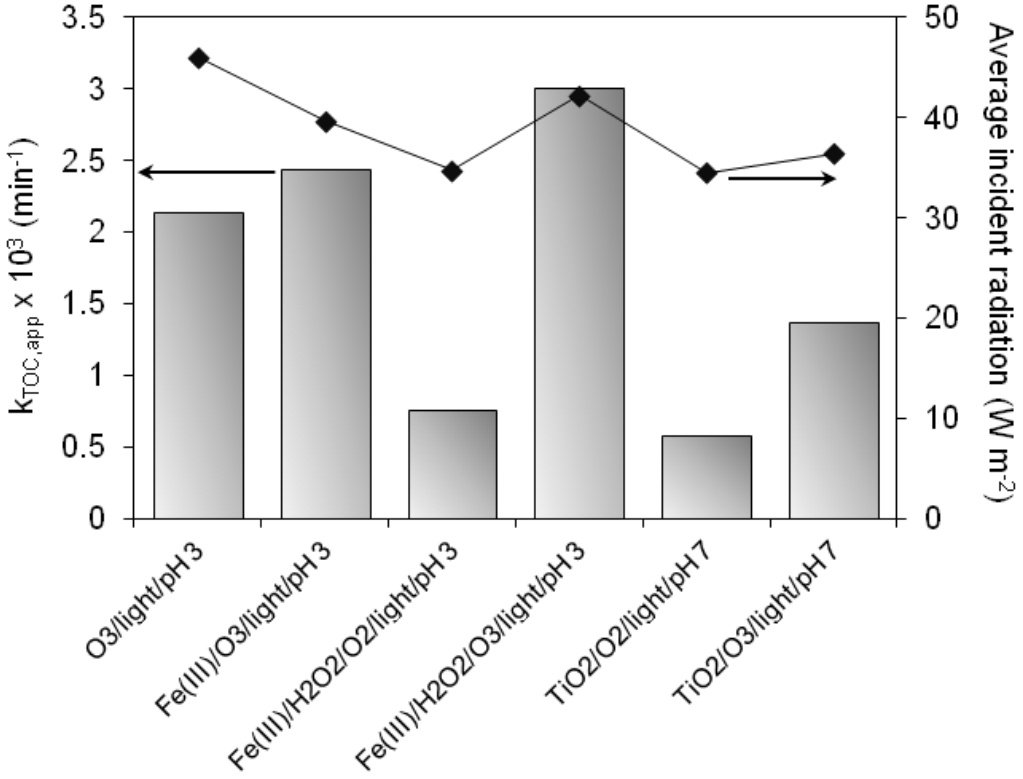

Fig.5. Apparent mineralization rate constant and average incident radiation for some experiments. Experimental conditions: EC concentration= 200 µg L^{-1}, each; Applied ozone = 520 mg h^{-1}; $C_{Fe(III),0}$ = 2.8 mg L^{-1}; Initial H_2O_2/Fe/(III) mass ratio = 6.1; $C_{TiO2,0}$ = 200 mg L^{-1}.

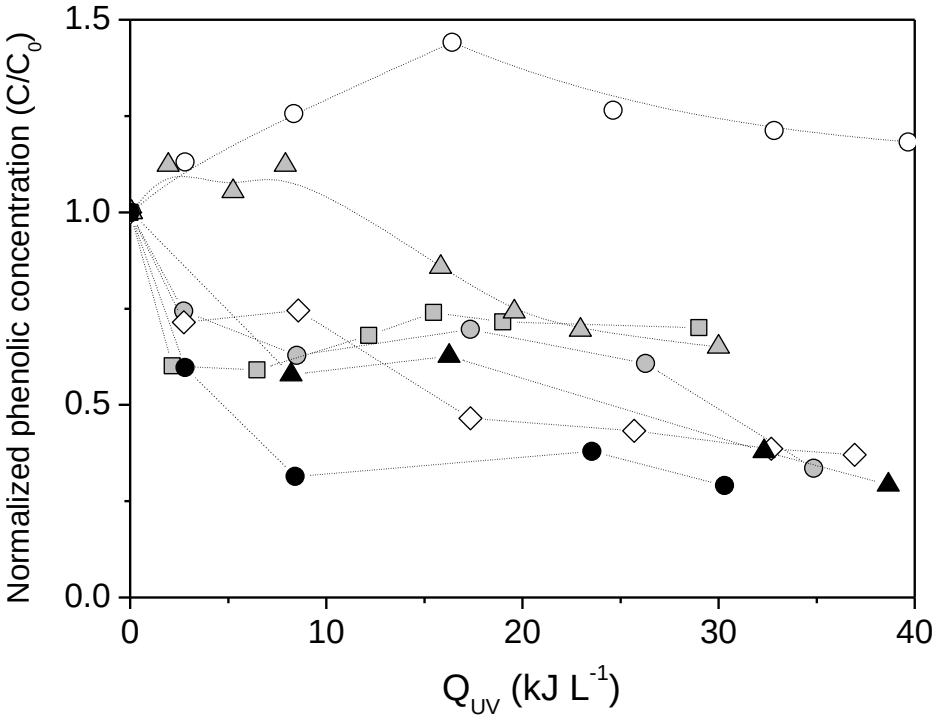

Fig.6. Evolution of the phenolic concentration with the dose of UV radiation during the course of some photocatalytic experiments. Experimental conditions: EC concentration= 200 μg L^{-1}, each; Applied ozone = 520 mg h^{-1}; $C_{Fe(III),0}$ = 2.8 mg L^{-1}; Initial H_2O_2/Fe/(III) mass ratio = 6.1; $C_{TiO2,0}$ = 200 mg L^{-1}. Symbols: (◍) O_3/light/pH 3, (○) Fe(III)/O_2/light/pH 3, (◇) Fe(III)/O_3/light/pH 3, (▣) Fe(III)/H_2O_2/O_2/light/pH 3, (▲) Fe(III)/H_2O_2/O_3/light/pH 3,(△) TiO_2/O_2/light/pH 7, (●) TiO_2/O_3/light/pH 7